Room-temperature ferromagnetism of Mn-doped InAs by a diffusion treatment

SHAN DONG[*], FENG ZHU, GUANDONG YANG
State Key Laboratory for Superlattices and Microstructures, Institute of Semiconductors, Chinese Academy of Sciences, P. O. Box 912, Beijing 100083, China

InAs crystal wafer showing ferromagnetism have been successfully synthesized by diffusing Mn into InAs under a high-temperature annealing. The concentration of Mn in crystal is 7.8% calculated from X-ray diffraction (XRD) pattern. The sample shows a clear ferromagnetic hysteresis loops at room-temperature, and Curie temperature (T_C) may be above 300K. The hole concentration of InAs wafer increases from 2.38×10^{17} cm^{-3} to 2.51×10^{17} cm^{-3} after Mn is doped into InAs, which may originate from the replacement of In iron by Mn iron. Our first-principle calculations confirm that the ferromagnetic ordering of *p*-type InMnAs sample is due to strong *p-d* exchange interaction and hole-mediated ferromagnetism.

1. Introduction

Diluted magnetic semiconductors (DMSs), combining with transport and ferromagnetic properties into the same material and thereby opening up a path to entirely new devices, have attracted a great deal of attentions in the last two decades [1-10]. DMS with Curie temperature (T_C) above room temperature is required for various spin-dependent devices. Therefore the main challenge of experiments is how to improve Curie temperature T_C of DMS. Although $Ga_{1-x}Mn_xAs$ [11-14] and $In_{1-x}Mn_xAs$ [15-22] are extensively studied as pioneering DMSs with long-range ferromagnetic ordering, up to date, the highest Curie temperature T_C of $Ga_{1-x}Mn_xAs$ is about 191K with heavily doped Mn in GaAs ($x = 0.2$) [14]. In the case of InAs, Munekata *et al.* [15] succeeded in the growth of $In_{1-x}Mn_xAs$ thin film for the first time by molecular beam epitaxy (MBE) at low temperatures of about 200~300 ^{o}C. The first observation of ferromagnetism (FM) in *p*-type $In_{1-x}Mn_xAs$ layer was reported [16], but the Curie temperature is very low ($T_C \leq 7K$). Then Koshihara *et al.* [17] enhanced the Curie temperature T_C up to 35K by using *p*-$In_{1-x}Mn_xAs$ /GaSb heterostructures grown by Molecular Beam Epitaxy (MBE). Slupinski *et al.* [18] reported FM $In_{1-x}Mn_xAs$ for $T_C = 50K$ with relatively low hole concentration and Mn composition. Schallenberg and Munekata [19] have grown $In_{1-x}Mn_xAs$ epilayers with a Curie temperature of 90K. In recent years, room temperature FM order of $In_{1-x}Mn_xAs$ thin film has been observed [20-22].

On the other hand, the origin of the FM in DMS is still under debate. Also, it is not clear whether Mn$_n$ clusters or secondary phases, such as MnAs, have formed in Mn-doped InAs or not. Theoretically, the band structure model [23-25], based on the *p-d* and *d-d* level repulsions between the TM ions and host elements, has been successfully used to explain the magnetic ordering observed in all Mn-doped III-V and II-VI semiconductors. In this model, the carriers (electrons or holes) play an important role in stabilizing the ferromagnetism of DMS. In order to confirm the model above, we have also performed first-principle calculations based on the local spin density approximations to study the magnetic properties of InAs:Mn system.

2. Experimental details

XRD is used to characterize the structure of samples by D/MAX 2500. The wavelength λ of the monochromatic X-ray beam is 1.5406$Å$ as and CuKa radiation is the X-ray laboratory source. Magnetization characterizations are acquired using a superconducting quantum interface device (SQUID) magneto-meter. The Hall measurement is carried out in order to determine the carrier concentration of *p*-type InAs diffused with Mn.

p-type InAs wafers grown by liquid encapsulated Czochralski (LEC) method which were used as the substrates in our experiments. The substrate is firstly purified by C_2HCl_3, CH_3COCH_3 and C_2H_5OH in sequence to get rid of the organics and then washed in HCl for cleaning minerals. After that, Mn is evaporated onto the surface of InAs utilizing pure tungsten boat as a heat source while the substrate is preserved under 2.8×10^{-3} Pa at room temperature. Then, the sample is immediately sealed up in a quartz envelope in vacuum. The annealing was carried out in a sealed quartz tube with a pressure of 2×10^{-3} Pa at 800℃ for 24 hours. Before we characterize InMnAs, HCl and de-

ionized water are used to clear the residual Mn and other impurities on the surface of the film.

3. Results and discussion

Table 1 shows that the hole concentration of Mn-doped InAs is increased from 2.38×10^{17} cm^{-3} to 2.51×10^{17} cm^{-3} after Mn doped into InAs. This increment may due to the replacement of In^{+3} by Mn^{+2}, which would reduce a hole in the system.

Table 1. The hole concentration and mobility of InAs with and without Mn doping at room temperature.

Sample	concentration	mobility
Mn-doped	$2.51 \times 10^{17} cm^{-3}$	$213.1 cm^2/V_s$
Mn undoped	$2.38 \times 10^{17} cm^{-3}$	$218.5 cm^2/V_s$

The structural characterization of InAs:Mn wafer is examined by X-ray diffraction system and XRD patterns of InAs and InMnAs are plotted in Fig. 1. A strong InMnAs (002) peak observed at $2\theta=29.55°$ is shown in Fig. 1(a). Comparing with the peaks of InAs(002) at $2\theta=29.54°$, it is clear that the peak central position shift slightly to higher angle. According to the position of the peak, The InMnAs lattice constant calculated (6.041 Å) is less than that of InAs (6.043 Å). The decrease of lattice constant could attribute to the replacement of In ions by Mn ions in InAs, because Pauling radius of Mn^{2+} (80pm) is less than that of In^{3+} (81pm). According to Vegard's law, the content of Mn is estimated to be about 8% in In$_{1-x}$Mn$_x$As as $\alpha_{InMnAs} = x\alpha_{MnAs}+(1-x) \alpha_{InAs}$ where α_{MnAs} is the lattice constant of structure MnAs and the value reported is about 6.014 [15]. The concentration of Mn in the crystal is 7.8% calculated from X-ray diffraction (XRD) pattern. Moreover, no distinct peaks originating from other impurity phases such as MnAs were detected in Fig. 1(a).
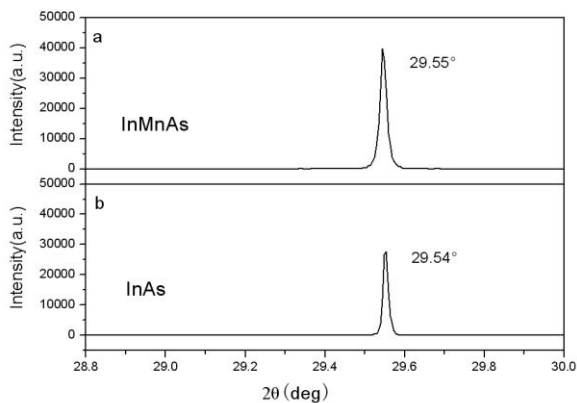
Fig. 1. θ-2θ X-ray diffraction pattern of InMnAs (a) and InAs (b).

The temperature-dependent magnetization (M-T) curve for single-phase Mn-doped InAs sample are meas-

ured using a SQUID magnetometer with a magnetic field of 1000Oe, applied perpendicular to the film plane. The dc zero-field-cooled (ZFC) and the field-cooled (FC) magnetization curves are shown in the insert of Fig. 2. FC is up-curve, and ZFC is down-curve. Measurements are performed from 5 to 300K. The FC is obtained by measuring the magnetic moment of the sample in a magnetic field of 1000Oe during cooling. The ZFC measurement is obtained by first cooling the sample to 5 K in zero field and then warming it in the same field as that of the FC measurement. The ZFC magnetization shows stronger temperature dependence than the FC one which below 300 K. Above 300K the ZFC-FC curves still separate, the ferromagnetic ordering sets are shown clearly in inserts of Fig. 2. It can be explained that by the spins entering a frozen state below the blocking temperature the super-paramagnetic particle is in the blocked state, while the magnetic anisotropy overcomes the thermal activation energy. The insert of Fig. 2 displays a ferromagnetic behavior persisting above 300 K. Therefore, it obtains the Curie temperature T_C above 300 K in this system. As seen in Fig. 2 the sample displays ferromagnetic ordering and a very slowly decreases with increasing temperature.
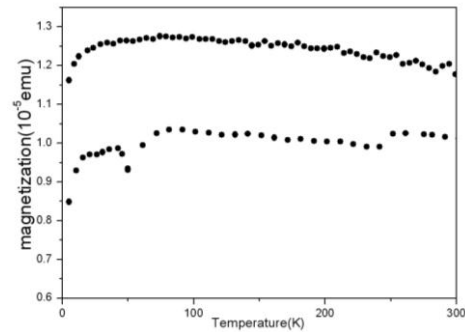
Fig. 2. Temperature-dependent magnetization curve of InMnAs measured by SQUID.

Fig. 3 shows that the measurement of hysteresis loops at 300K of the samples after subtracting the diamagnetic background. The well-defined hysteresis loops show the InAs:Mn wafer is clearly ferromagnetic ordering at room temperature. The coercive field (H$_c$) of this sample is 448 Oe. Remanent magnetization (M$_r$) and saturation magnetization (M$_s$) of the samples are 3.9 emu/cm^3 and 14.5 emu/cm^3, respectively. The absence of any detectable traces of secondary phases or Mn clusters from the Hall measurement and XRD results clearly confirms the ferromagnetic signal is not produced by secondary phases or clusters in the sample. These results agree that transitions related to neutral Mn acceptor are increasing in the same sample as described above. Ferromagnetic hysteresis loops enhance noticeably, which indicates that Mn-related bands are activated due to the supply of fluent holes from the neutral Mn. Such holes increase ferromagnetic exchange interactions.
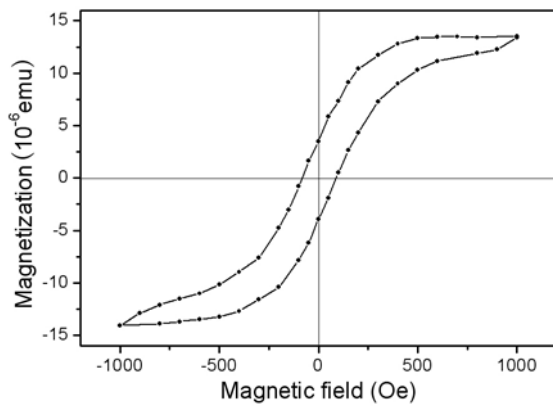
Fig. 3. Magnetic hysteresis-loop of InMnAs measured by SQUID at 300 K.

Fig. 4 Total, As-p, Mn-e, Mn-t_2 projected density of states (DOS) for Mn-doped in InAs. The black curves plot for spin-up states, and light gray curves for spin-down states. The vertical dashed line indicates the Fermi level at zero energy.

To further demonstrate that the Mn-doped InAs crystals are favorable for high temperature ferromagnetism, we model 64-atom cell to simulate the magnetic interactions of Mn atoms. The calculations are performed using VASP code [27], based on the spin density functional theory [28, 29]. For the exchange and correlation potential, the generalized gradient approximation (GGA) is used [30]. All plane waves with a cutoff energy of 300 eV are used in the basis function. For all the Mn-doped systems, a 64 atoms supercell is used for the defect calculations. The lattice constants of the supercells are kept fixing to that of pure InAs. All the ion positions are allowed to relax until the forces on each of them become less than $0.02 eV/Å$. For ion relaxation, a $2\times2\times2$ Monkhost-Pack k-point sampling is used [31].

Fig. 4 shows the calculated total and projected density of states (DOS) for Mn-doped InAs while Mn substitutes In. When Mn is doped in cubic InAs, it creates Mn-t_{2d} and e_d majority spin (spin-up) states below valence band maximum (VBM), while minority states above VBM. Strong coupling between the As-p orbital and Mn-t_{2d} orbital can be seen in Fig. 4 because the Mn-t_{2d} state has the same symmetry as the VBM As-p state. It clearly represents that the majority t_2 and e states are under Fermi level, while minority states above. It results in a magnetic moment in Mn-doped bulk InAs. In terms of p-d band coupling model, ferromagnetic (FM) repulsion between majority mixing of As-p and Mn-t_{2d} states results in net energy gain because of the unfilled anti-bonding p-d states. In addition, more holes in this system will enhance the FM ordering. Therefore, the magnetic ground state is FM, not antiferromagnetic (AFM) state. The calculated total energy differences between FM and AFM configuration ($\Delta E = E_{FM} - E_{AFM}$) are -181 meV, indicating that ferromagnetic ordering is favorable for InAs:Mn system. Therefore, the observed ferromagnetism should be the intrinsic behavior of Mn-doped InAs. So, the p-d coupling dominates the magnetic ordering.
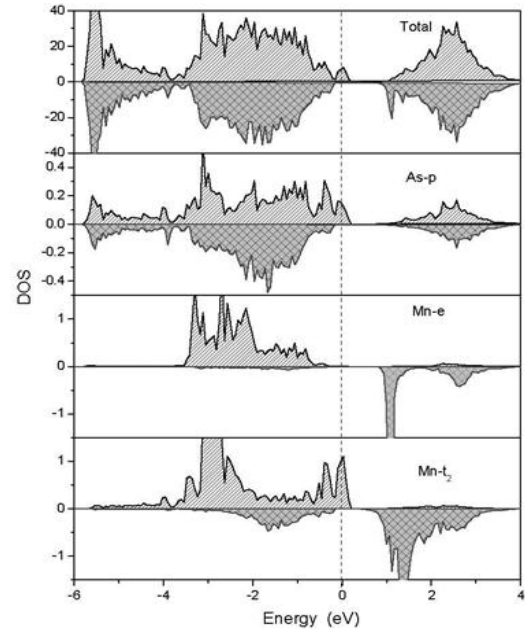
4. Conclusions

In summary, Mn doped InAs with high Curie temperature ferromagnetism has been successfully fabricated. The Mn concentration is very low. Hall measurements and XRD results reveal that the sample is crystallized with Mn ions substituted for In ions and no trace of secondary phases or clusters is detected. Magnetization measurements show clear ferromagnetic hysteresis loops in InAs:Mn crystal at room-temperature, and the Curie temperature Tc is above 300K. The first-principles calculations based on spin-polarized density functional theory confirm that the ferromagnetic ordering of p-type InAs:Mn sample is due to strong p-d exchange interaction and hole-mediated ferromagnetism.

Acknowledgements

References

[1] H. Ohno, Science **281**, 951 (1998).
[2] A. J. Mills, Nature (London) **392,** 147 (1998).
[3] S. A. Wolf, D. D. Awschalom, R. A. Buhrman, J. M. Daughton, S von Molnar, Science **294**, 1488 (2001).
[4] T. Dietl, H. Ohno, F. Matsukura, J. Cibert, D. Ferrand, Science **287**, 1019 (2000).
[5] J. M. D. Coey, M. Venkatesan, C. B. Fitzgerald Nature Mater. **4**, 173 (2005).

[6] A. Walsh, Juarez L. F., Da Silva, S.-H. Wei Phys. Rev. Lett. **100**, 256401 (2008).

[7] H. Saito, V. Zayets, S. Yamagata, K. Ando, Phys. Rev. Lett. **90**, 207202 (2003).

[8] H. Pan, J. B. Yi, L. Shen, R. Q. Wu, J. H. Yang, J. Y. Lin, Y. P. Feng, J. Ding, L. H. Van, J. H. Yin, Phys. Rev. Lett. **99**, 127201 (2007).

[9] H. Peng, H. J. Xiang, S. H. Wei, S. S. Li, J. B. Xia, J. B. Li, Phys. Rev. Lett. **102**, 017201 (2009).

[10] H. Peng, J. B. Li, S. S. Li, J. B. Xia, Phys. Rev. B **79**, 092411 (2009).

[11] H. Ohno, A. Shen, F. Matsukura, A. Oiwa, A. Endo, S. Katsumotoe, Appl. Phys. Lett. **69**, 363 (1996).

[12] D. Chiba, Y. Nishitani, F. Matsukura, H. Ohno, Appl. Phys. Lett. **90**, 122503 (2007).

[13] S. Mack, R. C. Myers, J. T. Heron, A. C. Gossard, D. D. Awschalom, Appl. Phys. Lett. **92**, 192502 (2008).

[14] L. Chen, S. Yan, P. F. Xu, J. Lu, W. Z. Wang, J. J. Deng, Appl. Phys. Lett. **95**, 182505 (2009).

[15] H. Munekata, H. Ohno, S. von Molnar, A. Segmuller, L. L. Chang, L Esaki, Phys. Rev. Lett. **63**, 1849 (1989).

[16] H. Munekata, H. Ohno, R. R. Ruf, R. J. Gambino, L. L. Chang, J. Cryst. Growth **111**, 1011 (1993).

[17] S. Koshihara, A. Oiwa, M. Hirasawa, S. Katsumoto, Y. Iye, C. Urano, H. Takagi, Phys. Rev. Lett. **78**, 4617 (1997).

[18] T. Slupinski, A. Oiwa, S. Yanagi, H. Munekata, J. Cryst. Growth **37**, 1326 (2002).

[19] T. Schallenberg, H. Munekata, Appl. Phys. Lett. **89**, 042507 (2006).

[20] A. J. Blattner, B. W. Wessels, Appl. Surf. Sci. **221**, 155 (2004).

[21] P. T. Chiu, B. W. Wessels, Phys. Rev. B **76**, 165201 (2007).

[22] R. Gonzalez-Arrabal, Y. Gonzalez, L. Gonzalez, M. Garcia-Hernandez, F. Munnik, M. S. Martin-Gonzalez, J. Appl. Phys. **105**, 073911 (2009).

[23] G. M. Dalpian, S. H. Wei. Solid State Commun **138**, 353 (2006).

[24] H. Peng, J. Li, S. S. Li, J. B. Xia, J. Phys. Condens. Matter **20**, 125207 (2008).

[25] X. Q. Meng, L. Tang, J. Li, J. Phys. Chem. C **114**, 17569 (2010).

[26] Semiconductors: Data Handbook, 3rd edition, edited by O. Madelung. Berlin: Springer (2004).

[27] G. Kresse, J. Hafner, Phys. Rev. B **48**, 13115 (1993).

[28] W. Kohn, L. J. Sham, Phys. Rev. B **140**, A1133 (1965).

[29] P. Hohenberg, W. Kohn, Phys. Rev. **136**, B864 (1994).

[30] J. P. Perdew, Y. Wang Phys. Rev. B **33**, 8800 (1986).

[31] H. J. Monkhorst, J. D. Pack. Phys. Rev. B **13**, 5188 (1976).

_____
[*]Corresponding author: dongshan08@semi.ac.cn